

# Intelligent Reflecting Surface-induced Randomness for mmWave Key Generation

Shubo Yang  
Glasgow College

University of Electronic Science and Technology of China  
Chengdu 611731, China  
2429400y@student.gla.ac.uk

Han Han

Electrical and Computer Engineering Department  
University of Toronto  
ON M5S 3G4, Canada  
johnny.han@mail.utoronto.ca

Yihong Liu

James Watt School of Engineering School of Aerospace, Transport and Manufacturing  
University of Glasgow Cranfield University  
Glasgow, U.K. Cranfield, U.K.  
y.liu.6@research.gla.ac.uk weisi.guo@cranfield.ac.uk

Weisi Guo

Lei Zhang

James Watt School of Engineering  
University of Glasgow  
Glasgow, U.K.  
lei.zhang@glasgow.ac.uk

**Abstract**—Secret key generation in physical layer security exploits the unpredictable random nature of wireless channels. However, the millimeter wave (mmWave) channels have limited multipath and may not be Gaussian distributed. In this paper, for mmWave secret key generation of physical layer security, we use intelligent reflecting surface (IRS) to produce randomness and induce artificial Rayleigh fading directly in the wireless environments. We first formulate the model of IRS-assisted key generation in mmWave environments. The IRS-assisted reflection channel varies according to the IRS weights' variation and induces randomness. When considering the IRS weights are continuous and discrete uniformly distributed, we find that the reflection channel variance is equal to the number of IRS elements. Besides, we prove that the magnitude and phase are Rayleigh and uniformly distributed when the weights are continuously and discretely distributed with more than one quantization bit. With the simulation results verifying the analytical results, this work explains the mathematical principles behind the IRS-assisted physical layer security secret key generation and lays a foundation for future mmWave key generation evaluation and optimization of channel randomness.

**Index Terms**—Physical layer security, secret key generation, intelligent reflecting surface, reconfigurable intelligent surface.

## I. INTRODUCTION

Wireless networks are becoming ubiquitous nowadays and in the future Internet of Things (IoT) systems. However, their broadcast nature makes them vulnerable to malicious attacks. Classic encryption schemes, such as advanced encryption standard and public key cryptography, are dependent on cryptography computation techniques [1]. The applications of classic schemes to IoT devices and wireless sensor networks (WSNs) bring challenges, since the devices and sensor nodes have small sizes and limited computational capability. Thus, extensive research is carried out in secret key generation in physical layer security [2], where the legitimate users extract keys from their correlated observations of the reciprocal channel in a lightweight manner [3]. The correlation of wireless channels makes it possible to generate keys without key

exchange, and the dynamic uniqueness of the channel between the transmitter and receiver prevents eavesdroppers mimicking. While in dynamic environments the movements of users or objects are sufficient to produce randomness, the randomness is limited in static environments, such as in open terrain with no moving objects.

Moreover, millimeter wave (mmWave) communication with huge bandwidth from 30 GHz to 300 GHz is envisioned a significant technology for the fifth generation (5G) networks [4]. However, most previous works focus on key generation in sub-6GHz systems [3] [5] and model on Gaussian channels [6] [7] instead of in mmWave systems. The mmWave channels has a poor scattering nature and exhibits limited multipath, so they may not conform to Gaussian channels. There is research on mmWave key generation [8] [9]. Virtual angle of arrival (AoA) and angle of Departure are used to generate a shared secret key between two devices [8], while a small perturbation angle is incorporated into the AoA of the transmitter as the common randomness to improve secrecy rate [9]. These abovementioned mmWave key generation methods induce randomness at the transmitter and receiver sides, which requires increased transmitter or receiver hardware complexity, and the additional hardware greatly raises the cost.

By incorporating the newly developed intelligent reflecting surface (IRS) (also known as RIS: Reconfigurable Intelligent Surface) that makes wireless channels controllable, the randomness will be generated directly in the wireless transmission channel and the hardware cost at transceivers will be significantly reduced. IRS is a two-dimensional surface consisting of a large number of passive low-cost reflecting elements [10]. Each scattering element of IRS is independently capable of altering the weights, i.e., amplitude and/or phase, of the incident signals. Additionally, IRS possesses several advantages, e.g., flexibly reconfigure the wireless channels, easy deployment due to its flexible shape, and sustainable implementations with its passive nature. By integrating IRS in

the environment, e.g., positioning IRS to a wall, IRS is able to realize smart radio environments. Besides, IRS becomes more important in high-frequency bands communications, e.g., mmWave and THz communications since they suffer from severe coverage issues, and the existing IRS applications mainly target at indoor scenarios with static or deterministic transmitters and receivers [11].

Thus, in this paper, through dynamically controlling the wireless channels, IRS offers an added degree of freedom to induce channel randomness in mmWave systems, without needing increased transceiver complexity. The key generation based on IRS-induced randomness also does not rely on dynamic environments, which overcomes the lack of randomness problem in static environments. To the best of authors' knowledge, this is the first paper researched into IRS-induced randomness for mmWave key generation. Moreover, we focus on the fundamental mathematical principles and analytical derivations of producing channel randomness in mmWave communications when giving random IRS weights. IRS weights are discrete practically, but continuous weights are the ideal case and the upper limit for discrete IRS weights when their quantization bit approaches to infinity. Thus, the controllable weight of each element is considered first as an ideal continuous and then a practical discrete uniformly-distributed random variable (r.v.). The IRS-assisted reflection channel is considered to be another r.v.. The relationship between the two variable distributions and the specific reflection channel distribution are revealed in this paper. To summarize, the main contributions of this paper are as follows.

- We establish a model of secret key generation using IRS as a channel randomness source in mmWave scenarios and represent the IRS-assisted reflection channel using steering vectors.
- The relationship between the continuous uniformly-distributed IRS weights and IRS-assisted reflection channel distribution is established when IRS is under uniform rectangular array (URA) configuration. The reflection channel distribution, variance, magnitude distribution, and phase distribution are derived. Through adding IRS, randomness and an artificial Rayleigh fading are induced in the environments.
- The reflection channel distribution for discretely uniformly-distributed URA IRS is derived, depending on the quantization bit. The reflection channel variance, magnitude distribution, and phase distribution are derived accordingly.

In this paper, bold-faced letters are used to denote matrix or column vectors, while lightfaced letters are used to denote scalar quantities. Superscripts  $(\cdot)^T$ ,  $(\cdot)^*$ , and  $(\cdot)^H$  represent the transpose, conjugate and conjugate transpose operations, respectively.  $\odot$  denotes the point-wise multiplication. We use the notations shown in Table I to describe our model, derivation and results.

TABLE I: Notations

Symbol	Definition
$\lambda$	Wavelength
$k$	Wave number, where $k = \frac{2\pi}{\lambda}$
$d$	Element spacing in IRS
$M$	Element number of the IRS
$m$	An integer in range $[1, M]$
$\phi_m$	The phase shift of the $m$ th IRS element weight
$\psi$	The incident or reflected azimuth angle
$\theta$	The incident or reflected elevation angle
$r$	The magnitude of the IRS-assisted reflection channel
$\beta$	The phase in radians of the IRS-assisted reflection channel
$B$	Indicates the IRS discrete weight quantization bit
$v$	Indicates the amplitude of direct path signal
$h_{(\cdot)}$	Indicates the channel
$U(a, b)$	Indicates a uniform distribution on interval $(a, b)$
$N(\mu, \sigma^2)$	Indicates a Gaussian distribution with mean $\mu$ and variance $\sigma^2$
$(\cdot)_x, (\cdot)_y$	Indicate physical quantities on $x$ -axis and $y$ -axis, respectively
$(\cdot)_{real}, (\cdot)_{imag}$	Indicate quantities of the real and imaginary parts, respectively
$(\cdot)_{cos}, (\cdot)_{sin}$	Indicate quantities of cosine and sine functions, respectively
$(\cdot)_i, (\cdot)_o$	Indicate incident and reflected angles, respectively
$(\cdot)_C, (\cdot)_D$	Indicate quantities when IRS weights are continuous and discrete, respectively

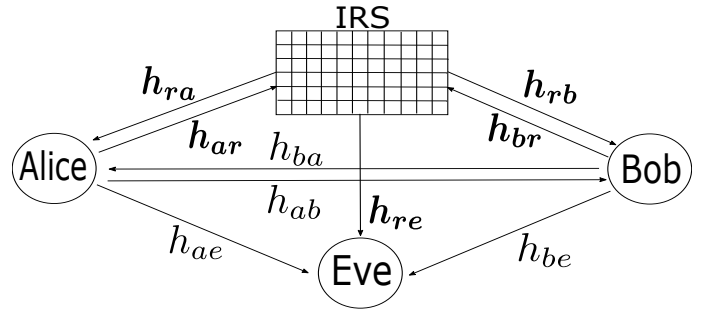


Fig. 1: IRS-assisted secret key generation model.

## II. SYSTEM MODEL

Consider an IRS-assisted wireless communication between one pair of legitimate parties, Alice and Bob. There is also an eavesdropper Eve, who passively listens to the communication between Alice and Bob. Assume all the parties are operated under a mmWave static environment, i.e., the legitimate parties and objects in the ambient environment do not move. Besides, the transmission is assumed far-field without fading. This assumption can be justified since the multipath effect is constrained and the high path loss makes non-line-of-sight paths' power small.

As shown in Fig. 1. Alice and Bob aim at establishing a random secret cryptographic key based on their reciprocal communication channel and reducing the key leakage to Eve. They measure the common channel through their exchanged signals and generate keys using parameters of the received signals, e.g. channel state information (CSI) and received signal strength (RSS). When Alice transmits signal  $s$ , the received signal at Bob can be expressed as

$$y = (h_{ab} + \mathbf{h}_{rb}^H \mathbf{W} \mathbf{h}_{ar})s + n, \quad (1)$$

where  $h_{ab} \in \mathbb{C}^{1 \times 1}$ ,  $\mathbf{h}_{ar} \in \mathbb{C}^{M \times 1}$ ,  $\mathbf{h}_{rb} \in \mathbb{C}^{M \times 1}$  represent the direct channel between Alice and Bob, the channel between Alice and IRS, and the channel between IRS and Bob,  $n$  is the additive white Gaussian noise (AWGN), and  $\mathbf{W}$  is the diagonal weight matrix with each entity on the diagonal being the IRS weight of each surface element. The weight

of the  $m_{th}$  surface element is represented as  $e^{j\phi_m}$ , where  $\phi_m \in [0, 2\pi)$ . Since the transmission channel between Alice and Bob is reciprocal, we only consider the situation that Alice is transmitting signals to Bob to avoid redundancy. Additionally, since path loss is a coefficient related to distance and can be easily predicted by eavesdropper [12], we discuss the randomness and channel distribution without path loss.

To generate shared keys in static environments and reduce the key leakage to Eve, it is crucial to increase the channel randomness through IRS. As in (1), though  $\mathbf{h}_{ar}$  and  $\mathbf{h}_{rb}$  are static in mmWave static environments, when IRS weights  $\mathbf{W}$  vary,  $\mathbf{h}_{rb}^H \mathbf{W} \mathbf{h}_{ar}$  becomes dynamic. Thus, IRS becomes the major source of channel randomness through varying the reflection channel  $\tilde{H} = \mathbf{h}_{rb}^H \mathbf{W} \mathbf{h}_{ar}$ . In this case, we focus on  $\tilde{H}$ , which can be expressed using steering vectors and weight vector [13] as

$$\tilde{H} = \mathbf{w}^H \cdot [\mathbf{a}(\boldsymbol{\Omega}_i) \odot \mathbf{a}(\boldsymbol{\Omega}_o)] , \quad (2)$$

where  $\mathbf{w}$  is the weight vector with each entity being the diagonal entity of  $\mathbf{W}$ , i.e., weight of each surface element. Besides, the steering vector of the channels between Alice and IRS and between IRS and Bob are

$$\mathbf{a}(\boldsymbol{\Omega}_i) = [a(\boldsymbol{\Omega}_{i,1}), \dots, a(\boldsymbol{\Omega}_{i,m}), \dots, a(\boldsymbol{\Omega}_{i,M})]^T \quad (3)$$

$$\mathbf{a}(\boldsymbol{\Omega}_o) = [a(\boldsymbol{\Omega}_{o,1}), \dots, a(\boldsymbol{\Omega}_{o,m}), \dots, a(\boldsymbol{\Omega}_{o,M})]^T , \quad (4)$$

where  $\boldsymbol{\Omega}_{i,m}$  and  $\boldsymbol{\Omega}_{o,m}$  are the terms characterizing the incident spatial information from Alice at  $m_{th}$  element of IRS and the reflected spatial information from  $m_{th}$  element to Bob, respectively. Since the environment is static, then  $\boldsymbol{\Omega}_i$  and  $\boldsymbol{\Omega}_o$  are fixed, and  $\tilde{H}$  becomes a function of solely IRS weight vector  $\mathbf{w}$ . Note that averaging  $\tilde{H}$  derived from all possible pairs of  $\boldsymbol{\Omega}_i$  and  $\boldsymbol{\Omega}_o$  provides an estimation of the overall reflection channel distribution.

### III. IRS-ASSISTED REFLECTION CHANNEL DISTRIBUTION

In this section, we focus on the unknown relationship between the weight distribution and the reflection channel distribution. In detail, we derive the probability density function (p.d.f) of reflection channel  $\tilde{H}$  with given continuous and discrete uniformly-distributed URA IRS weights. Assume the distributions of IRS weight phase shifts  $\{\phi = [\phi_1, \dots, \phi_m, \dots, \phi_M], m \in [1, M]\}$  are independent and identically distributed (i.i.d). Note that uniform linear array (ULA) can be considered as a special case of URA while URA is a typical uniform planar array structure. Thus, we consider IRS in URA configuration, which can be further extended into other complex IRS shapes.

#### A. Reflection Channel Assisted by Continuously Distributed IRS

Assume that the IRS weight phase shifts  $\phi$  are continuous uniformly distribution  $\phi_m \sim U(0, 2\pi)$ , with p.d.f  $\{f(\phi_m) = \frac{1}{2\pi}, \phi_m \in [0, 2\pi)\}$ . Consider a URA IRS with  $M_x$  and  $M_y$  elements equally spaced on x-axis and y-axis, respectively, where the total element number is  $M = M_x \cdot M_y$ . The

incident and reflected angles are described by  $\boldsymbol{\Omega}_i = (\psi_i, \theta_i)$  and  $\boldsymbol{\Omega}_o = (\psi_o, \theta_o)$ . The multiplication of steering vectors in (2) with elements spacing along x-axis  $d_x$  and y-axis  $d_y$  can be expressed as

$$\mathbf{a}(\boldsymbol{\Omega}_i) \odot \mathbf{a}(\boldsymbol{\Omega}_o) = [1, e^{j(\xi_x \cdot 1 + \xi_y \cdot 0)}, \dots, e^{j(\xi_x \cdot (m_x - 1) + \xi_y \cdot (m_y - 1))}, \dots, e^{j(\xi_x \cdot (M_x - 1) + \xi_y \cdot (M_y - 1))}]^T , \quad (5)$$

where  $m_x \in [1, M_x]$  and  $m_y \in [1, M_y]$  are integers [14]. Additionally,

$$\xi_x = kd_x (\cos \psi_i \sin \theta_i + \cos \psi_o \sin \theta_o) , \quad (6)$$

$$\xi_y = kd_y (\sin \psi_i \sin \theta_i + \sin \psi_o \sin \theta_o) . \quad (7)$$

Consequently, the reflection channel following (2) can be constructed as

$$\begin{aligned} \tilde{H} &= 1 + e^{j[\phi_2 + (\xi_x \cdot 1 + \xi_y \cdot 0)]} + \dots + e^{j[\phi_m + (\xi_x \cdot (m_x - 1) + \xi_y \cdot (m_y - 1))]} \\ &\quad + \dots + e^{j[\phi_M + (\xi_x \cdot (M_x - 1) + \xi_y \cdot (M_y - 1))]} \\ &= \sum_{m_y=1}^{M_y} \sum_{m_x=1}^{M_x} e^{j[\phi_m + (m_x - 1) \cdot \xi_x + (m_y - 1) \cdot \xi_y]} \\ &= \sum_{m_y=1}^{M_y} \sum_{m_x=1}^{M_x} e^{j(\phi_m + \alpha)} , \end{aligned} \quad (8)$$

where

$$m = (m_y - 1) \cdot M_x + m_x , \quad (9)$$

$$\alpha = (m_x - 1) \cdot \xi_x + (m_y - 1) \cdot \xi_y . \quad (10)$$

According to the central limit theorem (CLT),  $\tilde{H}$  converges to a complex Gaussian distribution when  $M$  is large enough. This assumption could be justified since a practical IRS usually has an extremely large number of elements, e.g. more than tens of elements [11]. By Euler's formula,  $\tilde{H}$  is further expanded as follows.

$$\tilde{H} = \sum_{m_y=1}^{M_y} \sum_{m_x=1}^{M_x} \cos(\phi_m + \alpha) + j \sum_{m_y=1}^{M_y} \sum_{m_x=1}^{M_x} \sin(\phi_m + \alpha) . \quad (11)$$

Therefore, the real and imaginary parts both converge to Gaussian distributions that are fully determined by means and variances. The mean and variance of the real part of  $\tilde{H}$ ,  $\mu_{real,C}$  and  $\sigma_{real,C}^2$ , can be expressed as

$$\mu_{real,C} = \mathbb{E} \left[ \sum_{m_y=1}^{M_y} \sum_{m_x=1}^{M_x} \cos(\phi_m + \alpha) \right] = \sum_{m_y=1}^{M_y} \sum_{m_x=1}^{M_x} \mu_{cos,C} \quad (12)$$

$$\sigma_{real,C}^2 = \sigma^2 \left[ \sum_{m_y=1}^{M_y} \sum_{m_x=1}^{M_x} \cos(\phi_m + \alpha) \right] = \sum_{m_y=1}^{M_y} \sum_{m_x=1}^{M_x} \sigma_{cos,C}^2 , \quad (13)$$

where  $\mu_{cos,C}$  and  $\sigma_{cos,C}^2$  are the mean and variance of  $\cos(\phi_m + \alpha)$ , functions of  $\{m_x, m_y\}$  and  $\{\xi_x, \xi_y\}$ , and can

be calculated as follows.

$$\mu_{\cos,C} = \int_0^{2\pi} \cos(\phi_m + \alpha) f(\phi_m) d\phi_m . \quad (14)$$

$$\sigma_{\cos,C}^2 = \int_0^{2\pi} \cos^2(\phi_m + \alpha) f(\phi_m) d\phi_m - \mu_{\cos,C}^2 . \quad (15)$$

(14) takes the integral of one period of  $\phi_m \in [0, 2\pi)$  with equal probability of  $f(\phi_m) = \frac{1}{2\pi}$ , so  $\mu_{\cos,C} = 0$  and consequently  $\sigma_{\cos,C}^2 = \frac{1}{2}$ .  $\mu_{\cos,C}$  and  $\sigma_{\cos,C}^2$  remain constant, so they are independent of the values of  $\{m_x, m_y\}$  and  $\{\xi_x, \xi_y\}$ . The mean and variance of the real part of  $\tilde{H}$  become

$$\mu_{\text{real},C} = M\mu_{\cos,C} = 0 \quad (16)$$

$$\sigma_{\text{real},C}^2 = M\sigma_{\cos,C}^2 = \frac{M}{2} . \quad (17)$$

Similarly, for the imaginary part of  $\tilde{H}$ , the mean and variance  $\mu_{\text{imag},C}$  and  $\sigma_{\text{imag},C}^2$  are determined by  $\mu_{\sin,C} = 0$  and  $\sigma_{\sin,C}^2 = \frac{1}{2}$ .

Hence,  $\tilde{H}$  is a complex Gaussian r.v. with real part and imaginary part being  $N(0, \frac{M}{2})$ . The distribution of  $\tilde{H}$  is also independent of  $\Omega_i$  and  $\Omega_o$ .

With any pair of incident and reflected angles, the mean of  $\tilde{H}$  is  $\mu_C = 0$  while the variance of  $\tilde{H}$  can be calculated as

$$\sigma_C^2 = \mathbb{E}[(\tilde{H} - \mu_C)(\tilde{H} - \mu_C)^*] = \mathbb{E}[\tilde{H}\tilde{H}^*] = M . \quad (18)$$

Due to the channel parameters CSI and RSS are normally used to generate keys, we further derive the magnitude and phase distributions. Since the real and imaginary parts of  $\tilde{H}$  constitute a joint Gaussian distribution and the correlation of them equals to 0, the real and imaginary parts are independent. According to the joint Gaussian distribution, the result magnitude p.d.f  $f_r(r)$  and phase p.d.f  $f_\beta(\beta)$  of  $\tilde{H}$  are Rayleigh and uniform distributions as follows.

$$f_r(r) = \begin{cases} \frac{2r}{M} e^{-\frac{r^2}{M}}, & r \geq 0 \\ 0, & r < 0 \end{cases} \quad (19)$$

$$f_\beta(\beta) = \begin{cases} \frac{1}{2\pi}, & \beta \in [0, 2\pi) \\ 0, & \text{otherwise} \end{cases} \quad (20)$$

Note that (19) and (20) show that the continuous uniformly distributed weight produce an artificial Rayleigh fading and randomness for the reflection channel. When the direct path and reflection path are both considered, the induced Rayleigh fading will turn into Rician fading since the direct path adds a non-zero mean on the reflection path [15]. The magnitude conforms to the Rician fading p.d.f expressed as

$$f_r(r) = \begin{cases} \frac{2r}{M} e^{-\frac{(r^2+v^2)}{M}} I_0\left(\frac{2rv}{M}\right), & r \geq 0 \\ 0, & r < 0 \end{cases} \quad (21)$$

where  $I_0(\cdot)$  is the modified Bessel function of the first kind with order zero, and  $v$  is the amplitude of the signal from direct path.

## B. Reflection Channel Assisted by Discretely Distributed IRS

Assume IRS has discrete weight phase shifts  $\phi$ , with quantization bit  $B$ . Then  $\phi_m$  is uniformly distributed on discrete values  $\{0, \frac{2\pi}{2^B}, \dots, \frac{2\pi(2^B-1)}{2^B}\}$ . When the  $B$  approaches to infinity, the channel approaches to the ideal distribution when IRS has continuous weights.

Similarly to the continuous distributed IRS case, the reflection channel can be expanded as in (11) and converges to a complex Gaussian distribution. The mean and variance of the real part are similar as in (12) (13).  $\mu_{\cos,D}$  and  $\sigma_{\cos,D}^2$  are expressed as

$$\mu_{\cos,D} = \mathbb{E}\{\cos(\phi_m + \alpha)\} , \quad (22)$$

$$\sigma_{\cos,D}^2 = \mathbb{E}\{\cos^2(\phi_m + \alpha)\} - \mu_{\cos,D}^2 . \quad (23)$$

Since for discrete uniformly distributed  $\phi$ ,  $\mu_{\cos,D} = 0$ , then  $\sigma_{\cos,D}^2$  can be expressed as

$$\begin{aligned} \sigma_{\cos,D}^2 &= \frac{1}{2} + \frac{1}{2} \mathbb{E}\{\cos(2\phi_m + 2\alpha)\} \\ &= \frac{1}{2} + \frac{1}{2} \cos(2\alpha) \mathbb{E}\{\cos(2\phi_m)\} - \frac{1}{2} \sin(2\alpha) \mathbb{E}\{\sin(2\phi_m)\}, \end{aligned} \quad (24)$$

where the means of  $\cos(2\phi_m)$  and  $\sin(2\phi_m)$  determine  $\sigma_{\cos,D}^2$ .

When  $B \geq 2$ ,  $\mathbb{E}\{\cos(2\phi_m)\} = 0$  and  $\mathbb{E}\{\sin(2\phi_m)\} = 0$ , which leads to  $\sigma_{\cos,D}^2 = \frac{1}{2}$ . Therefore, same as the continuous case, the channel is a Gaussian complex random variable with real and imaginary parts being  $N(0, \frac{M}{2})$ . The variance, magnitude and phase are the same as in (18) (19) (20).

When  $B = 1$ ,  $\mu_{\text{real},D} = \mu_{\text{imag},D} = 0$ . Different from  $B \geq 2$  case, since  $\phi_m$  only takes values  $\{0, \pi\}$ ,  $\mathbb{E}\{\cos(2\phi_m)\} = 1$  and  $\mathbb{E}\{\sin(2\phi_m)\} = 0$ . Thus,  $\sigma_{\cos,D}^2 = \frac{1}{2} + \frac{1}{2} \cos(2\alpha)$ , and the variances of the real and imaginary parts of  $\tilde{H}$  can be expressed as

$$\sigma_{\text{real},D}^2 = \frac{M}{2} + \frac{1}{2} \sum_{m_y=1}^{M_y} \sum_{m_x=1}^{M_x} \cos(2\alpha) , \quad (25)$$

$$\sigma_{\text{imag},D}^2 = \frac{M}{2} - \frac{1}{2} \sum_{m_y=1}^{M_y} \sum_{m_x=1}^{M_x} \cos(2\alpha) . \quad (26)$$

The independence between the real and imaginary parts of  $\tilde{H}$  also does not hold. The covariance  $\mathbf{R}$  between them are expressed as

$$\begin{aligned} \mathbf{R} &= \mathbb{E}\left\{ \sum_{m_y=1}^{M_y} \sum_{m_x=1}^{M_x} \cos(\phi_m + \alpha) \sin(\phi_m + \alpha) \right\} \\ &= \sum_{m_y=1}^{M_y} \sum_{m_x=1}^{M_x} \frac{1}{2} \cos(2\alpha) \mathbb{E}\{\sin(2\phi_m)\} + \frac{1}{2} \sin(2\alpha) \mathbb{E}\{\cos(2\phi_m)\} \\ &= \sum_{m_y=1}^{M_y} \sum_{m_x=1}^{M_x} \frac{1}{2} \sin(2\alpha) . \end{aligned} \quad (27)$$

The derivation of the magnitude and phase distributions turns into deriving the envelop and phase of correlated Gaussian

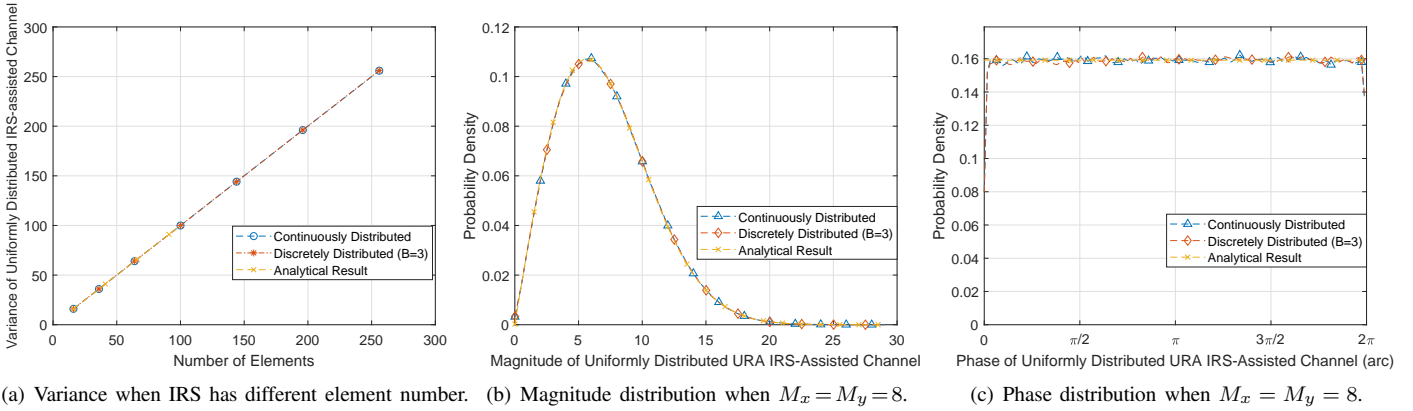


Fig. 2: The variance, magnitude distribution and phase distribution of the reflection channel assisted by URA IRS with continuous and discrete (quantization bit  $B = 3$ ) uniformly distributed weight.

quadratures according to [15]. The reflection channel variance is not affected by the dependence, being same as (18).

#### IV. SIMULATION RESULTS

##### A. Verification for Continuously Distributed IRS

1) *IRS-Assisted Reflection Channel Variance*: Set  $d = \frac{\lambda}{2}$ ,  $\Omega_i = (30^\circ, 30^\circ)$ , and  $\Omega_o = (150^\circ, 60^\circ)$ .  $M_x$  and  $M_y$  are set to 4 at first, and then increased to 16 by 2 at a time. Thus,  $M$  increases from 16 to 256. The simulation for the reflection channel variance with respect to  $M$  is plotted in Fig. 2(a). The variances of  $\bar{H}$  are equal to the square of  $M_x$  and increase linearly with  $M$ , which proves (18). The simulation results of Fig. 2(a) verify that, as the number of elements grow, the IRS has a great potential to induce channel variations since it is usually implemented with huge number of elements.

2) *Magnitude and Phase Distributions*: Set  $M = 64$ , with  $M_x = M_y = 8$ , while other parameters remain unchanged. The magnitude and phase distributions are presented in Fig. 2(b) and Fig. 2(c), respectively. As the graphs show, the magnitude and phase distribution simulation results match the analytical results (19) (20) very well, that are, a Rayleigh distribution and a uniform distribution being independent of  $\Omega_i$  and  $\Omega_o$ , respectively. Note that the sharp drops around 0 and  $2\pi$  in Fig. 2(c) result from several adjacent probability density values outside the bound  $[0, 2\pi)$ , being equal to 0, are averaged to plot a smoother p.d.f. The simulation results of channel parameters in Fig. 2(b) and Fig. 2(c) show the IRS-induced variation of IRS. The independence of the reflection channel distribution of  $\Omega_i$  and  $\Omega_o$  means that whatever angles Alice and Bob locate in, the channel randomness remains the same for generating keys. Additionally, the channel Eve receives stays unchanged and no more information leakage dependent on angles. Note that if Eve locates in the same angle as Bob and nearer to Alice than Bob, the information is fully leaked. This is because in the far-field environment, Eve and Bob are differentiated solely by their locating angles. However, the probability of such situation happening can make it be ignored. The uniform phase distribution means that

the values in  $[0, 2\pi)$  are taken with equal probability. Thus, when CSI is utilized to generate keys, it greatly prevents Eve guessing the particular phase of the channel between Alice and Bob. Moreover, besides ideal continuous uniformly-distributed weights, it is natural to further extend the conclusions to other distributions, which will be our future work.

##### B. Verification for Discretely Distributed IRS

1) *IRS Weight Quantization Bit  $B \geq 2$* : Set  $B = 3$ . Other parameters remain the same as the continuous case. The simulations for the variance, magnitude, and phase of the reflection channel are plotted in Fig. 2(a) Fig. 2(b) Fig. 2(c). The simulation results match the ideal continuous weight case and the analytical results. This means that the ideal channel distribution and uniform phase distribution can be achieved under a more practical situation, i.e.  $B \geq 2$ .

2) *IRS Weight Quantization Bit  $B = 1$* : Set  $B = 1$ , and two pairs of input and output angles, with case 1:  $\Omega_i = (30^\circ, 30^\circ)$ ,  $\Omega_o = (150^\circ, 60^\circ)$ , and case 2:  $\Omega_i = (110^\circ, 50^\circ)$ ,  $\Omega_o = (310^\circ, 20^\circ)$ . Other parameters are the same as continuous case. The simulation for the reflection channel variance is plotted in Fig. 3(a), where the variances increase proportionally with respect to  $M$ . The real and imaginary part of the reflection channel for two cases when  $M_x = M_y = 8$  are plotted in Figure. 3(b) and Figure. 3(c), respectively. The simulation results match the analytical results well, and the zero means of the two parts and the variances in (25) (26) are verified. Note that the real and imaginary part variances are dependent on values of  $\Omega_i$  and  $\Omega_o$ . Additionally, when  $B = 1$ , the ideal channel distribution in Section IV-A and uniform channel phase distribution cannot be achieved, which shows the limitation of 1 quantization bit.

#### V. CONCLUSIONS

This paper utilizes IRS for mmWave physical layer security secret key generation, and completes the analytical channel distribution derivation and the underlying mathematical principles. Though mmWave channels lack scattering and multipath, the IRS induces randomness and an artificial Rayleigh fading

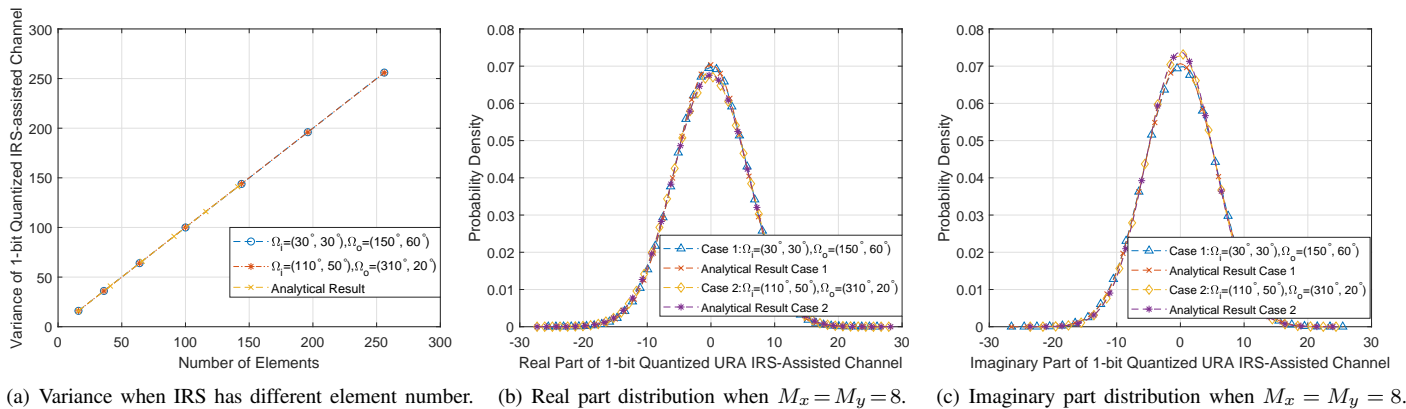


Fig. 3: The variance, real part distribution and imaginary part distribution of the reflection channel assisted by URA IRS with discrete uniformly distributed weight (quantization bit  $B = 1$ ).

so as to realize channel encryption in a static environment. Specifically, based on the IRS-assisted secret key generation model, we consider URA IRS weights as continuous and discrete uniformly distributed variables and IRS-assisted reflection channel as another variable. The relationship between the two variables and the reflection channel distribution are derived. Additionally, we find that the reflection channel converges to a complex Gaussian distribution, and the reflection channel variance is equal to the number of elements. When the weights are continuous and discrete uniformly distributed with quantization bit larger than one, the magnitude and phase distributions are Rayleigh and uniform distributions, respectively. Our theoretical conclusions are verified by simulations.

## REFERENCES

- [1] J. Zhang, S. Rajendran, Z. Sun, R. Woods, and L. Hanzo, "Physical layer security for the internet of things: Authentication and key generation," *IEEE Wireless Communications*, vol. 26, no. 5, pp. 92–98, 2019.
- [2] J. Zhang, T. Q. Duong, A. Marshall, and R. Woods, "Key generation from wireless channels: A review," *IEEE Access*, vol. 4, 2016.
- [3] J. Zhang, R. Woods, T. Q. Duong, A. Marshall, Y. Ding, Y. Huang, and Q. Xu, "Experimental study on key generation for physical layer security in wireless communications," *IEEE Access*, vol. 4, pp. 4464–4477, 2016.
- [4] A. M. Al-samman, M. H. Azmi, and T. A. Rahman, "A survey of millimeter wave (mm-wave) communications for 5g: Channel measurement below and above 6 ghz," in *Recent Trends in Data Science and Soft Computing*, F. Saeed, N. Gazem, F. Mohammed, and A. Busalim, Eds. Cham: Springer International Publishing, 2019, pp. 451–463.
- [5] K. Moara-Nkwe, Q. Shi, G. M. Lee, and M. H. Eiza, "A novel physical layer secure key generation and refreshment scheme for wireless sensor networks," *IEEE Access*, vol. 6, pp. 11 374–11 387, 2018.
- [6] J. W. Wallace and R. K. Sharma, "Automatic secret keys from reciprocal mimo wireless channels: Measurement and analysis," *IEEE Transactions on Information Forensics and Security*, vol. 5, no. 3, pp. 381–392, 2010.
- [7] J. Wallace, "Secure physical layer key generation schemes: Performance and information theoretic limits," in *2009 IEEE International Conference on Communications*, 2009, pp. 1–5.
- [8] L. Jiao, J. Tang, and K. Zeng, "Physical layer key generation using virtual aoa and aod of mmwave massive mimo channel," in *2018 IEEE Conference on Communications and Network Security (CNS)*, 2018, pp. 1–9.
- [9] L. J. et al., "Secret beam: Robust secret key agreement for mmwave massive mimo 5g communication," in *2018 IEEE Global Communications Conference (GLOBECOM)*, 2018, pp. 1–6.
- [10] Q. Wu, S. Zhang, B. Zheng, C. You, and R. Zhang, "Intelligent reflecting surface aided wireless communications: A tutorial," *IEEE Transactions on Communications*, pp. 1–1, 2021.
- [11] S. Gong, X. Lu, D. T. Hoang, D. Niyato, L. Shu, D. I. Kim, and Y.-C. Liang, "Toward smart wireless communications via intelligent reflecting surfaces: A contemporary survey," *IEEE Communications Surveys Tutorials*, vol. 22, no. 4, pp. 2283–2314, 2020.
- [12] X. Hu, L. Jin, K. Huang, X. Sun, Y. Zhou, and J. Qu, "Intelligent reflecting surface-assisted secret key generation with discrete phase shifts in static environment," *IEEE Wireless Communications Letters*, vol. 10, no. 9, pp. 1867–1870, 2021.
- [13] Y. Liu, L. Zhang, B. Yang, W. Guo, and M. A. Imran, "Programmable Wireless Channel for Multi-user MIMO Transmission using Meta-surface," in *2019 IEEE Global Communications Conference*, 2019, pp. 1–6.
- [14] H. Han, Y. Liu, and L. Zhang, "On half-power beamwidth of intelligent reflecting surface," *IEEE Communications Letters*, pp. 1–1, 2020.
- [15] V. A. Aalo, G. P. Efthymoglou, and C. Chayawan, "On the envelope and phase distributions for correlated gaussian quadratures," *IEEE Communications Letters*, vol. 11, no. 12, pp. 985–987, 2007.